

## Electron delocalization and the characterization of the $L_3MM$ Auger spectra of 3d transition metals

Lo I Yin and Tung Tsang\*

Code 691, Astrochemistry Branch, Laboratory for Extraterrestrial Physics, NASA Goddard Space Flight Center, Greenbelt, Maryland 20771

Isidore Adler

Department of Chemistry, University of Maryland, College Park, Maryland 20742

(Received 18 October 1976)

The  $L_3M_{23}M_{23}$ ,  $L_3M_{23}M_{45}$ , and  $L_3M_{45}M_{45}$  Auger spectra of metals with both open and filled 3d bands are presented and analyzed in detail. From these experimental data it is possible to derive two parameters, a hole localization parameter  $\lambda_d$  and an energy parameter  $\Delta\epsilon$ , which can completely characterize the Auger spectra of the entire 3d transition-metal series.  $\lambda_d$  gives the quantitative extent of the delocalization of the 3d electrons in metals with unfilled 3d bands. Through a knowledge of  $\lambda_d$  it becomes possible to quantitatively evaluate the contributions of (i) the hole-hole interaction and (ii) the relaxation, to the total energy difference  $\Delta\epsilon$  between single- and double-hole final states. Furthermore these parameters are correlated with the quasiautomic vs band characteristics of Auger electrons.

### I. INTRODUCTION

Recently, a number of investigators<sup>1-9</sup> have observed and commented on the quasiautomic behavior of the  $XVV$  ( $X$ , inner shell;  $V$ , valence band) Auger spectra in metals with filled  $d$  bands such as Cu and Zn. Although the Auger electrons originate from the valence  $d$  bands of these metals, their Auger spectra show no evidence of band structure, but rather exhibit free-atom features with sharp peaks similar to Kr, Xe gases<sup>10,11</sup> as well as Zn and Cd vapors.<sup>12,13</sup> This is in sharp contrast to the alternative mode of deexcitation by soft-x-ray emission where the observed photon widths clearly include the occupied valence band.<sup>14,15</sup> The quasiautomic behavior of these metal Auger spectra has been interpreted as the withdrawal of electrons from the valence band (and hence localization) owing to the two-hole final state of Auger transitions as well as the preferential selection of these localized electrons through the short-range Auger operator  $1/r_{ij}$ .<sup>3,5</sup>

On the other hand, valence- and conduction-band features have been reported in the literature for the  $KVV$  Auger spectra of Be,<sup>16</sup> and C,<sup>17</sup> and for the  $L_{23}VV$  spectra of Al,<sup>5</sup> Mg,<sup>18</sup> and Si.<sup>19,20</sup> Apparently, the quasiautomic behavior of  $XVV$  Auger spectra is not universal for all metals. In fact, we<sup>21</sup> have observed band character in the  $L_3M_{45}M_{45}$  Auger spectra of V and Cr, consistent with the suggestion of Kowalczyk *et al.*<sup>22</sup> on the possibility of electron delocalization for unfilled 3d shells. In this paper, we specifically address ourselves

to this apparently ambivalent behavior (either quasiautomic or bandlike) of the Auger spectra in 3d transition metals and attempt to characterize it with experimentally measurable parameters.

So far, only the  $L_3M_{45}M_{45}$  Auger spectra of the metals with filled 3d shells have been analyzed in detail. For the present purpose we have studied in depth the complete series of Auger spectra including the  $L_3M_{23}M_{23}$ ,  $L_3M_{23}M_{45}$  transitions in addition to the  $L_3M_{45}M_{45}$  transitions of metals with both open and filled 3d bands. We shall show that from these experimental data, one may derive two empirical parameters, a hole localization parameter and an energy parameter<sup>21</sup> which can completely characterize the Auger spectra of the entire transition-metal series. The magnitudes of these parameters are correlated with the extent of quasiautomic behavior in these metals. Through these parameters one may also directly obtain an estimate of the total relaxation energies in the Auger process. Simple theoretical approximations of the relaxation energies will be given which are in reasonably good agreement with the experimental values. Recently Baro, Salmeron, and Rojo<sup>6,23</sup> have also studied the quasiautomic versus band behavior of Auger spectra using a different experimental approach. Rather than studying various transition metals with different final-state characteristics, they have studied the behavior of Auger spectra with different initial states by means of gas adsorbates. We note that the underlying physical ideas are rather similar, although our respective approaches are different from each other.

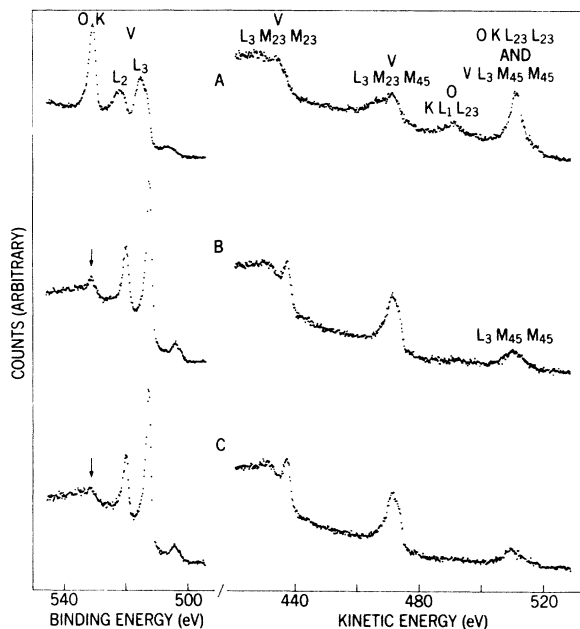


FIG. 1. Vanadium metal photoelectron spectra (left) and Auger spectra (right). (a) Before argon ion sputter cleaning. (b) After initial argon ion sputter cleaning. (c) After final sputter cleaning.

## II. EXPERIMENTAL

The x-ray photoelectron spectrometer was operated in a vacuum of  $\sim 1 \times 10^{-8}$  Torr. Magnesium  $K\alpha_{1,2}$  x rays were used for excitations. The Auger electrons were analyzed using a hemispherical electrostatic spectrometer of 11-cm radius. To achieve high resolution (Gaussian full width at half-maximum of  $\sim 0.4$  eV), the Auger electrons were retarded to  $\sim 60$  eV before entering the spectrometer. Electrons were pulse counted and their energy distribution was recorded with a multi-channel analyzer in the multiscaler mode.

The samples were spectroscopically pure metal foils, except for Cr, which was vacuum deposited on an aluminum substrate. Sample surfaces were sputter cleaned with argon ions at approximately 1.5 kV, 0.2 mA/cm<sup>2</sup>, and 0.002-Torr pressure until the oxygen  $K(1s)$  and carbon  $K$  photoelectron peaks either disappeared or showed a minimum intensity above background. The Fermi level was calibrated against the gold- and zinc-metal photoelectron spectra of Shirley<sup>24</sup> and of Ley *et al.*<sup>25</sup>

## III. RESULTS

In order to ascertain the quasiatomic or band behavior of Auger electrons we choose to compare the  $L_3M_{45}M_{45}$  spectra of vanadium and chromium with those of copper and zinc. This is because the

final Auger state of Cr ( $3d^2$ ) is configuratively equivalent to that of Cu and Zn ( $3d^9$ ), and the final state of V is  $3d^1$ . Experimentally, however, several difficulties arise. Both Cr and V are rather active metals whose surfaces are easily oxidized. It is difficult to remove the oxygen even by prolonged ion-sputter cleaning. Furthermore, the intensity of the  $L_3M_{45}M_{45}$  transition is quite low owing to the small number of  $d$  electrons. Nevertheless, as will be shown below, it is possible to obtain the correct spectra and the correct interpretation with a minimum of ambiguities.

The vanadium photoelectron and Auger spectra are shown in Fig. 1. It is seen that the oxygen  $KL_{23}L_{23}$  Auger transition has almost identical energies with the vanadium  $L_3M_{45}M_{45}$  transition, hence interfering strongly with the vanadium spectrum. The sequence A, B, and C shows the progressive cleaning of the metal surface by argon-ion bombardment. For the uncleaned metal foil (A), the oxygen  $K$ -photoelectron peak and the oxygen  $KL_1L_{23}$  Auger peak are quite prominent and one expects a strong contribution to the V  $L_3M_{45}M_{45}$  peak owing to the O  $KL_{23}L_{23}$  Auger transition. In the cleaning sequence B and C, although the oxygen  $K$ -photoelectron peak is significantly weaker in C as compared to B, the same degree of change is not observed in the intensity of the Auger peak of interest (V  $L_3M_{45}M_{45}$ —kinetic energy  $\sim 510$  eV). From this, one may conclude that the interference due to oxygen impurity is rather minimal for C.

Similarly, the sputter-cleaned chromium photoelectron and Auger spectra are shown in Fig. 2. Here, although the oxygen  $K$ -photoelectron peak is stronger than in the case of V, the  $KLL$  Auger transition energy of oxygen is sufficiently different from chromium to cause no interference.

In Fig. 3, the  $L_3M_{45}M_{45}$  Auger and the  $M_{45}$  band photoelectron spectra of V and Cr are compared with those of Cu and Zn. (Note: The V and Cr spectra are on a coarser energy scale than the Cu and Zn spectra.) The following features are noteworthy.

(a) The structures of  $L_3M_{45}M_{45}$  spectra of Cu and Zn are very similar to each other (both with  $3d^8$  final-state configuration), in spite of the pronounced difference in their valence-band photoelectron spectra.

(b) The observed  $L_3M_{45}M_{45}$  linewidths of Cu and Zn are distinctly narrower than their photoelectron bandwidths even when the contribution to the photoelectron width from the incident Mg  $K\alpha$  radiation ( $\sim 0.8$  eV) is taken into consideration. (The Auger linewidth is of course independent of the incident x-ray width, and the instrumental broadening is constant for both Auger and photo-

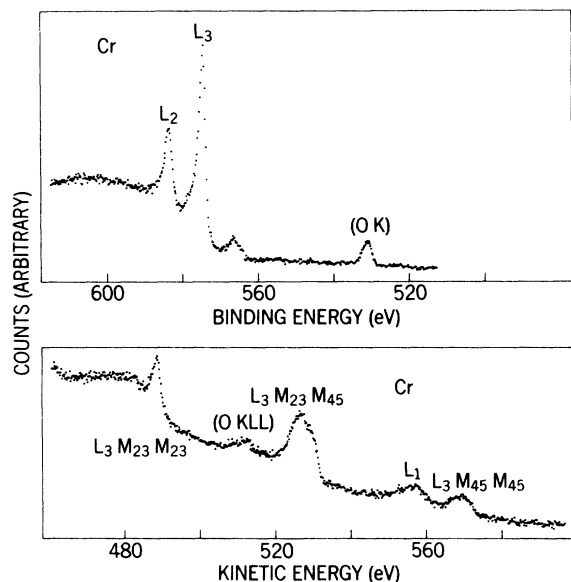


FIG. 2. Chromium metal photoelectron spectra (top) and Auger spectra (bottom). " $L_1$ " is the photoelectron peak from the  $L_1$  shell of Cr.

electron spectra.) This is in sharp contrast to the expected self-convolution of the  $M_{45}$  bandwidths in the  $L_3 M_{45} M_{45}$  spectra.

(c) The line shapes and line splittings of Auger spectra for solid Zn are distinctly similar to the Zn vapor spectra of Aksela *et al.*<sup>12</sup> where solid-state and band effects are absent.

(d) On the other hand, the behaviors of V and Cr are quite different. For V the Auger final-state configuration is  $3d^1$ , hence one would not expect the presence of any  $LS$ -coupling multiplets. Yet the observed V  $L_3 M_{45} M_{45}$  width (independent of the Mg  $K\alpha$  width) is larger than its  $M_{45}$  photoelectron

bandwidth (including the Mg  $K\alpha$  width). For Cr the Auger final state is  $3d^2$  which is configurationally equivalent to that of Cu and Zn ( $3d^8$ ). As can be seen from Fig. 3, not only are the  $LS$  multiplet structures missing in the  $L_3 M_{45} M_{45}$  spectrum of Cr but its width is also much broader than the  $M_{45}$  photoelectron band. It should be noted that in comparing the widths of  $L_3 M_{45} M_{45}$  spectra one should also include the widths of the  $L_3$  level. The measured  $L_3$  widths for Cu and Zn are 0.54 and 0.66 eV, respectively.<sup>26</sup> The observed  $L_3$  photoelectron widths of V and Cr (not shown) are also comparable to those of Cu and Zn (which is to be expected owing to the similarity in atomic number  $Z$  and the absence of Coster-Kronig transitions). Thus the  $L_3$  contribution to all the  $L_3 M_{45} M_{45}$  spectra shown in Fig. 3 can be considered to be negligible.

From (a)–(d), one may conclude that whereas the  $L_3 M_{45} M_{45}$  spectra of Cu and Zn are clearly quasiatomic in character, those of V and Cr definitely do not exhibit quasiatomic behavior.

In order to better understand the effect of unfilled  $3d$  shells on the Auger spectra involving  $3d$  electrons, the complete  $L_3 M_{23} M_{23}$ ,  $L_3 M_{23} M_{45}$ , and  $L_3 M_{45} M_{45}$  spectra for Fe, Co, Ni, Cu, and Zn are shown in Fig. 4. We observe that:

(a) With decreasing atomic number  $Z$ , beginning with Ni which has unfilled  $3d$  shells, the  $L_3 M_{45} M_{45}$  peak becomes very much broader compared to Cu and Zn (filled  $3d$  shells).

(b) In contrast, the characteristic structure of the  $L_3 M_{23} M_{45}$  group remains essentially unchanged throughout the transition-metal series.

(c) The  $L_3 L_{23} M_{23}$  Auger transition does not involve valence-band ( $3d$ ) electrons directly. Therefore one expects their behavior to be essentially atomic. One observes that although the coarse two-peak structure remains the same throughout the series, there is a definite improvement in the

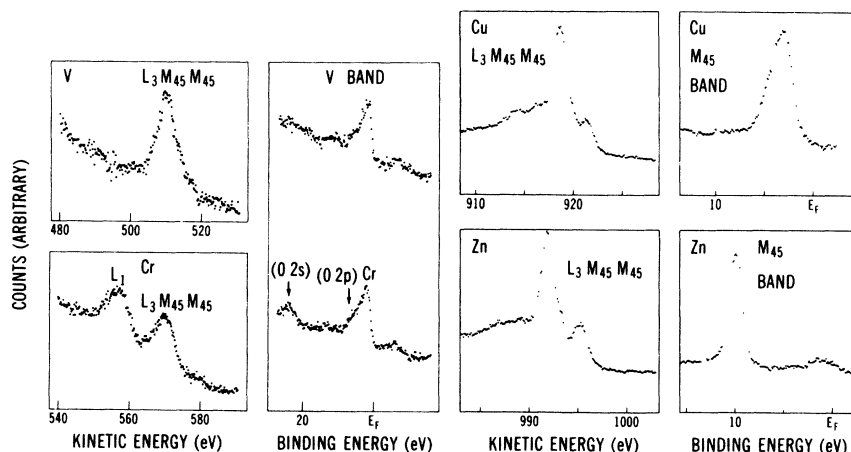


FIG. 3.  $L_3 M_{45} M_{45}$  Auger spectra and valence-band photoelectron spectra of V and Cr (left half) compared with those of Cu and Zn (right half). Note the coarser energy scale for V and Cr.

resolution of the two peaks as well as a sharpening of one of them with decreasing  $Z$ .

(d) With decreasing  $Z$ , the splitting between the two components of the  $L_3M_{23}M_{45}$  group decreases faster than that of the  $L_3M_{23}M_{23}$  group.

#### IV. EMPIRICAL CHARACTERIZATION OF THE AUGER SPECTRA

It is possible to systematically characterize the various features exhibited by the Auger spectra shown in Figs. 3 and 4 by introducing two experimentally measurable parameters. The physical significance of these parameters and their derivation will be discussed below.

##### A. Energy parameter

We<sup>21</sup> have previously introduced an energy parameter  $\Delta\epsilon(ijk)$  defined as:

$$\Delta\epsilon(ijk) = [B(i) - B(j) - B(k)] - K(ijk), \quad (1)$$

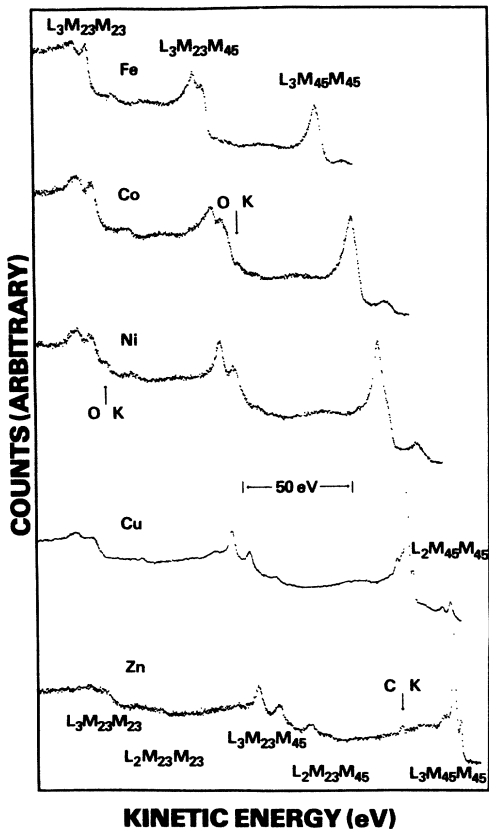


FIG. 4.  $L_{2,3}M_{23}M_{23}$ ,  $L_{2,3}M_{23}M_{45}$ , and  $L_{2,3}M_{45}M_{45}$  Auger spectra. From left to right, the ranges of kinetic energies are: Fe, 575–720 eV; Co, 630–800 eV; Ni, 690–875 eV; Cu, 759–943 eV; Zn, 805–1004 eV.

TABLE I. Energy parameters.

Z	Metal	$\Delta\epsilon(L_3M_{23}M_{23})$ (eV)	$\Delta\epsilon(L_3M_{23}M_{45})$ (eV)	$\Delta\epsilon(L_3M_{45}M_{45})$ (eV)
23	V	4.1 (1.0)	2.0 (1.0)	0 (0.8)
24	Cr	3.6 (1.0)	2.5 (1.0)	1.3 (0.8)
26	Fe	7.1 (0.8)	4.3 (1.0)	2.6 (0.8)
27	Co	8.0 (0.8)	6.4 (1.0)	3.7 (0.8)
28	Ni	7.0 (0.8)	8.0 (1.0)	5.3 (0.8)
29	Cu	9.4 (1.5)	12.6 (0.5)	8.6 (0.3)
30	Zn	10.8 (1.5)	13.3 (0.5)	10.5 (0.3)

where  $B(i)$  is the experimental binding energy of the  $i$ th shell observed from x-ray photoelectron spectroscopy, and  $K(ijk)$  is the experimental  $ijk$  Auger kinetic energy in a metal, both relative to its Fermi level. The first term  $B(i) - B(j) - B(k)$  is the *hypothetical* single-hole final-state kinetic energy of the  $ijk$  Auger transition whereas  $K(ijk)$  is the *observed* double-hole final-state kinetic energy. Since the energy parameter essentially measures the difference between two kinetic energies from the same sample, it is independent of the reference level and other sample-related experimental and systematic uncertainties. Furthermore this parameter contains the total effects of intra-, inter-, and extraatomic relaxation, and is independent of the manner in which these effects are partitioned. It gives a physically realistic estimate of the net difference in relaxation between single- and double-hole final states as well as hole-hole interactions. Thus, qualitatively, large values of  $\Delta\epsilon$  imply large changes in the valence-electron energy due to ineffective screening, high probability of withdrawal of electrons from the valence band during Auger emission, high degree of localization of electrons, and large likelihood of free-atom behavior. Using  $\Delta\epsilon$  for the  $L_3M_{45}M_{45}$  transition we<sup>21</sup> have qualitatively accounted for the bandlike character of Cu and Zn in contrast to the bandlike character of V and Cr shown in Fig. 3. Later, with the introduction of a second experimental parameter, it will be shown that quantitative evaluations of these effects are possible.

The measured values of  $\Delta\epsilon$  in eV for all three groups of Auger transitions ( $L_3M_{23}M_{23}$ ,  $L_3M_{23}M_{45}$ , and  $L_3M_{45}M_{45}$ ) are listed in Table I. The experimental uncertainties are given in parentheses. In  $L_3M_{23}M_{23}$  and  $L_3M_{23}M_{45}$  transitions where there are two prominent peaks of approximately equal intensity, the kinetic energy  $K(ijk)$  of the transition is taken to be the average of the two peaks. It should be noted that our  $\Delta\epsilon$  can be simply related to similar parameters introduced by other authors<sup>6,22,27-29</sup> under various contexts.

## B. Hole localization parameter

As mentioned before, although  $\Delta\epsilon$  gives a qualitative characterization of the behavior of  $L_3M_{45}M_{45}$  Auger spectra, it alone cannot provide quantitative information because it is a consequence not only of the net difference in relaxations between single- and double-hole final states but also hole-hole interaction. We shall introduce an experimentally derived hole localization parameter  $\lambda$  which is governed only by the actual strength of hole-hole interaction in the metal and is essentially independent of relaxations.

To arrive at this localization parameter  $\lambda$  we note that in free atoms such as Kr with totally localized electrons, the  $L_3M_{23}M_{23}$  and  $L_3M_{23}M_{45}$  Auger spectra are dominated by two prominent peaks within each group,<sup>10</sup> very similar to those shown in Fig. 4. The splitting  $S$  between the two peaks represents the strength of the atomic hole-hole interaction in the Auger final state and is related to the atomic Slater integrals. For example, the splitting  $S_{pp}$  between the two prominent peaks  $^1D$  and  $^3P$  in the  $L_3M_{23}M_{23}$  Auger group is governed by the Slater integral  $F^2(3p, 3p)$ .<sup>30</sup> For the  $L_3M_{23}M_{45}$  Auger group the assignment of the two prominent peaks are less certain.<sup>1,10,27,31</sup> If one adopts the assignments of ( $^1P, ^1F$ ) for the low-energy and ( $^3P, ^3D$ ) for the high-energy peaks which agree well with the theoretically predicted intensities,<sup>31,32</sup> then the splitting  $S_{pd}$  in this case is governed by the integrals  $G^1(3p, 3d)$ ,  $F^2(3p, 3d)$ , and  $G^3(3p, 3d)$ . From physical grounds one expects the ratio  $S_{pd}/S_{pp}$  for each element to remain essentially constant over a limited range of atomic number  $Z$ . This is indeed shown to be the case from the Hartree-Fock calculations of Mann.<sup>33</sup> Because  $S$  measures the difference in kinetic energy between two terms of the same Auger final state from the same sample, all relaxation effects cancel, and  $S$  is a function only of hole-hole interactions. In the  $3d$  transition-metal series, the

$3p$  ( $M_{23}$ ) electrons are fairly tightly bound with binding energies between 30 and 90 eV, so that  $3p$  holes can be considered as completely localized. This assumption is further supported by the agreement between the observed and theoretical (free-atom) trend of  $S_{pp}$  as a function of  $Z$ . Assuming  $3p$  holes are localized, then the deviation of  $S_{pd}/S_{pp}$  from a constant ratio can be considered to be a consequence of the delocalization of the  $3d$  hole. Furthermore, since experimentally we know that the Auger spectrum of metallic Zn ( $3d^{10}$ ) is free-atom like<sup>2</sup> and shows identical structures with identical splittings as that of Zn vapor (our Fig. 3 may be compared with the Zn vapor spectrum of Aksela *et al.*<sup>12</sup>), it is reasonable to assume complete localization of the  $3d$  holes in Zn. For  $Z > 30$  (Zn),  $3d$  levels have become corelike, thus one can also assume complete localization of the  $3d$  holes. In fact, using our Zn data and the As ( $Z = 33$ ) and Se ( $Z = 34$ ) data of Roberts, Weightman, and Johnson,<sup>27,31</sup> we find that  $S_{pd}/S_{pp}$  for all three elements are indeed identical to within experimental error (see Table II). Therefore, it is convenient to define and normalize the localization parameter  $\lambda_d$  (subscript indicating  $d$  hole) in the following way:

$$\lambda_d = \frac{S_{pd}/S_{pp}}{(S_{pd}/S_{pp})_{Zn, As, Se}} = \frac{1}{1.23} \frac{S_{pd}}{S_{pp}}. \quad (2)$$

We have  $\lambda_d = 1$  for Zn, As, and Se ( $Z \geq 30$ ) and  $0 \leq \lambda_d \leq 1$  for other metals with  $Z < 30$  and unfilled  $d$  shells.  $\lambda_d < 1$  signifies a hole-hole interaction weaker than that of two completely localized (free-atom like) holes, and hence, delocalization. Recently Citrin *et al.*<sup>34</sup> have also discussed the interaction between nonlocalized holes in the context of interatomic Auger transitions in ionic compounds. We emphasize that  $\lambda_d$  is completely empirical. The measured values (in eV) of  $S_{pp}$ ,  $S_{pd}$ , and  $\lambda_d$  are listed in Table II, with the experimental uncertainties given in parentheses. Figure

TABLE II. Localization parameters.

$Z$	Metal	$S_{pp}$ (eV)	$S_{pd}$ (eV)	$S_{pd}/S_{pp}$	$\lambda_d$
23	V	6.8 (1.0)	2.4 (0.6)	0.35 (0.16)	0.28 (0.10)
24	Cr	6.8 (1.5)	3.0 (0.5)	0.44 (0.20)	0.35 (0.11)
26	Fe	6.1 (0.6)	4.4 (0.5)	0.72 (0.11)	0.57 (0.13)
27	Co	6.9 (0.8)	4.8 (0.5)	0.69 (0.13)	0.55 (0.14)
28	Ni	7.0 (0.8)	6.4 (0.5)	0.91 (0.13)	0.72 (0.14)
29	Cu	7.5 (1.0)	8.0 (0.5)	1.07 (0.15)	0.85 (0.17)
30	Zn	7.6 (1.0)	9.6 (0.5)	1.26 (0.15)	1.23 (0.16)
33 <sup>a</sup>	As	9.7 (0.5)	11.7 (0.5)	1.21 (0.10)	
34 <sup>b</sup>	Se	10.0 (0.5)	12.2 (0.5)	1.22 (0.10)	

<sup>a</sup>Reference 31.<sup>b</sup>Reference 27.

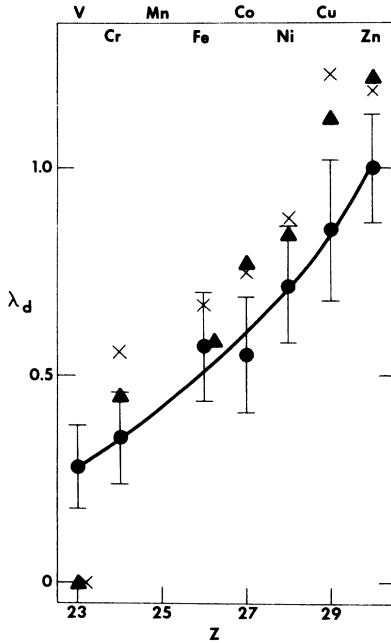


FIG. 5. Hole localization parameter  $\lambda_d$  vs atomic number  $Z$ . Filled circles, derived from experiment; filled triangles, calculated from  $\Delta\epsilon(L_3 M_{45} M_{45})$  and optical data; crosses, calculated from  $\Delta\epsilon(L_3 M_{45} M_{45})$  and theoretical  $\Delta\epsilon^2$  of Gelius and Siegbahn. Calculated values are systematically higher than experiment indicating overestimation of the localization of  $3d$  holes.

5 graphically shows the variation of  $\lambda_d$  as a function of  $Z$ . It is evident that  $\lambda_d$  is very small for V and Cr where the  $3d$  band is far from being filled. This high degree of delocalization of the  $3d$  hole, and by implication, highly efficient screening, is consistent with the presence of the band structure in the Auger spectra of V and Cr (Fig. 3).

### C. Empirical changes in relaxation energies

Using the two empirical parameters  $\Delta\epsilon$  and  $\lambda_d$ , it is now possible to quantitatively characterize the Auger spectra in Figs. 3 and 4. The energy parameter as defined in Eq. (1) can be written

$$\begin{aligned} \Delta\epsilon(ijk) &= [B(i) - B(j) - B(k)] - K(ijk) \\ &= [B(i) - B(j) - B(k)] - [B(i) - B^*(jk)] \\ &= B^*(jk) - [B(j) + B(k)] \\ &= B^*(jk) - B(jk). \end{aligned} \quad (3)$$

Here  $B^*(jk)$  indicates the effective combined binding energies of  $j$  and  $k$  electrons in the double-hole final Auger state and  $B(jk) = B(j) + B(k)$ . The kinetic energy  $K(ijk)$  of the Auger electron is frequently written as  $B(i) - B(j) - B^*(k)_j$ , where

$B^*(k)_j$  indicates the binding energy of the  $k$  electron in the presence of the  $j$  hole. Although convenient, physically this is somewhat artificial since it considers the Auger emission as a two-step process, i.e., first, the filling of the  $i$  hole by the  $j$  electron and then the  $k$  electron is ejected with an increased binding energy of  $B^*(k)_j$ , due to the presence of the  $j$  hole.

Actually the same Auger final state may also be reached by the ejection of the  $j$  electron with the  $k$  electron filling the  $i$  hole. Hence one might also expect that  $K(ijk) = B(i) - B^*(j)_k - B(k)$ . However, in a solid if  $j$  and  $k$  are from different shells (e.g., let  $j$  be inner shell,  $k$  be valence band), then the change in screening, and hence total relaxation, would be quite different between these two cases. Thus in general,

$$B(i) - B(j) - B^*(k)_j \neq B(i) - B^*(j)_k - B(k)$$

in a solid even though they describe the same Auger transition in this two-step representation. (Such problems do not arise for the special case of  $j = k$  as far as the kinetic energy is concerned.) Therefore we write  $K(ijk)$  as  $B(i) - B^*(jk)$  to indicate the interrelated character of the binding energies of  $j$  and  $k$  electrons due to the double-hole nature of the final Auger state.

Equation (3) then gives a physical representation of the energy parameter, that is, the net energy difference between double- and single-hole final states. The two components of this energy difference are hole-hole interaction and the total relaxation difference. Since the localization parameter is independent of the relaxation as mentioned earlier, we may write

$$\begin{aligned} \Delta\epsilon(ijk) &= B^*(jk) - B(jk) \\ &= \lambda_j \lambda_k F^0(j, k) - \Delta_R(j, k), \end{aligned} \quad (4)$$

where  $\Delta_R$  is the total relaxation difference between single- and double-hole final states and we have assumed that the Slater integral  $F^0$  to be the dominant term of the hole-hole interaction. Since  $\lambda_p = 1$ , we get

$$\Delta\epsilon(L_3 M_{23} M_{23}) = F^0(3p, 3p) - \Delta_R(3p, 3p), \quad (4a)$$

$$\Delta\epsilon(L_3 M_{23} M_{45}) = \lambda_d F^0(3p, 3d) - \Delta_R(3p, 3d), \quad (4b)$$

$$\Delta\epsilon(L_3 M_{45} M_{45}) = \lambda_d^2 F^0(3d, 3d) - \Delta_R(3d, 3d). \quad (4c)$$

In the last case,  $\lambda_d^2$  probably represents a lower limit, because the delocalization of the second  $d$  electron may be diminished somewhat as compared to the first  $d$  electron. From the values of  $\Delta\epsilon$  and  $\lambda_d$  in Tables I and II, we may use Eq. (4) to calculate  $\Delta_R$ . The results are listed as  $\Delta_R$  (obs.) in Tables III and IV.

It is interesting to note that for the inner-shell

TABLE III. Total relaxation energy differences in eV for  $L_3M_{45}M_{45}$  transition.  $\Delta_R(\text{obs.})$  are obtained from the experimental data using Eq. (4).  $\Delta_R(\text{calc.})$  are obtained from Eq. (10) by using  $\Delta_R^a$  from both optical data and the theoretical calculations of Gelius and Siegbahn as quoted in Ref. 22.

Z	Metal	$\Delta\epsilon(L_3M_{45}M_{45})$	$F^0(3d, 3d)$	$\lambda_d^2 F^0(3d, 3d)$	$\Delta_R(\text{obs.})$	$\Delta_R(\text{calc.})$	
						Opt.	Theor.
23	V	0	18.7	1.5	1.5	0.9	1.1
24	Cr	1.3	18.4	2.2	0.9	1.5	1.7
26	Fe	2.6	23.4	7.5	4.9	5.1	5.7
27	Co	3.7	24.8	7.4	3.7	5.6	5.5
28	Ni	5.3	26.3	13.7	8.4	9.7	10.1
29	Cu	8.6	26.0	18.7	10.1	13.9	14.7
30	Zn	10.5	29.1	29.1	18.6	22.1	21.7

transition  $L_3M_{23}M_{23}$  (Table IV),  $\Delta_R(\text{obs.})$  is large and does not decrease significantly with  $Z$  from Zn to V (23–20 eV). This implies a high degree of localization, large relaxation of outer electrons, both atomic and extra-atomic in the double-hole final state, and ineffective screening. This is in agreement with the observed free-atom character of this transition. In such cases the  $Z+1$  equivalent core approximation is probably valid. In contrast, for the  $L_3M_{45}M_{45}$  transition (Table III),  $\Delta_R(\text{obs.})$  decreases very rapidly with  $Z$  (19–1 eV), indicating much delocalization and very effective screening, bringing about band structure at low  $Z$ . In such cases of very effective screening the  $Z+1$  equivalent core approximation may not be valid. This behavior is graphically displayed in Fig. 6. As expected, the behavior of  $\Delta_R$  in the  $L_3M_{23}M_{45}$  transition (Table IV) is intermediate between the others (not shown in Fig. 6).

In Sec. V, semiempirical calculations of  $\lambda$  and  $\Delta_R$  will be given, and the calculated values may then be compared with the observed values.

## V. SEMIEMPIRICAL CALCULATIONS

### A. Localization parameter

We may also calculate the localization parameter using the experimental  $\Delta\epsilon$  values, and the appro-

priate atomic integrals and optical data. For a free atom in the frozen-orbital limit where the Koopmans theorem is assumed to be valid, and taking advantage of the fact that for the  $L_3M_{45}M_{45}$  transition the two  $3d$  electrons are equivalent, the energy parameter  $\Delta\epsilon(L_3M_{45}M_{45})$  simply becomes the Slater integral  $F^0$ :

$$\begin{aligned}\Delta\epsilon(L_3M_{45}M_{45}) &= B^*(3d, 3d) - B(3d, 3d) \\ &= B^*(3d) + B(3d) - 2B(3d) \\ &= B^*(3d) - B(3d) \\ &= F^0(3d, 3d).\end{aligned}\quad (5)$$

In reality, the atomic orbitals are different between the single- and double-hole final states. We denote the binding energy change as atomic relaxation<sup>35,36</sup>  $\Delta_R^a$ . Thus for free atoms,

$$B^*(3d) - B(3d) = F^0(3d, 3d) - \Delta_R^a.\quad (6)$$

In a metal, there is an additional difference in extra-atomic relaxation<sup>36</sup>  $\Delta_R^{\text{ea}}$  between single- and double-hole final states. Hence:

$$\begin{aligned}\Delta\epsilon(L_3M_{45}M_{45}) &= F^0(3d, 3d) - \Delta_R^a - \Delta_R^{\text{ea}} \\ &= F^0(3d, 3d) - \Delta_R.\end{aligned}\quad (7)$$

Here we have defined the total difference in relaxation  $\Delta_R$  as:

TABLE IV. Total relaxation energy differences in eV for  $L_3M_{23}M_{23}$  and  $L_3M_{23}M_{45}$  transitions.  $\Delta_R(\text{obs.})$  are obtained from the experimental data using Eq. (4).  $\Delta_R(\text{calc.})$  are obtained from the theoretical values of Gelius and Siegbahn as quoted in Ref. 22.

Z	Metal	$L_3M_{23}M_{23}$			$L_3M_{23}M_{45}$			
		$F^0(3p, 3p)$	$\Delta_R(\text{obs.})$	$\Delta_R^a(\text{theor.})$	$\Delta_R(\text{calc.})$	$F^0(3p, 3d)$	$\lambda_d F^0(3p, 3d)$	$\Delta_R(\text{obs.})$
23	V	24.0	19.9	7.8	16.7	21.0	5.9	3.9
24	Cr	25.2	21.6	8.8	17.2	21.2	7.4	4.9
26	Fe	28.4	21.3	10.6	20.5	25.6	14.6	10.3
27	Co	29.9	21.9	11.6	21.9	27.0	14.8	8.4
28	Ni	31.3	24.3	12.6	23.2	28.5	20.5	12.5
29	Cu	32.5	23.1	14.4	24.2	28.8	24.5	11.9
30	Zn	34.2	23.4	14.4	25.6	31.3	31.3	18.0

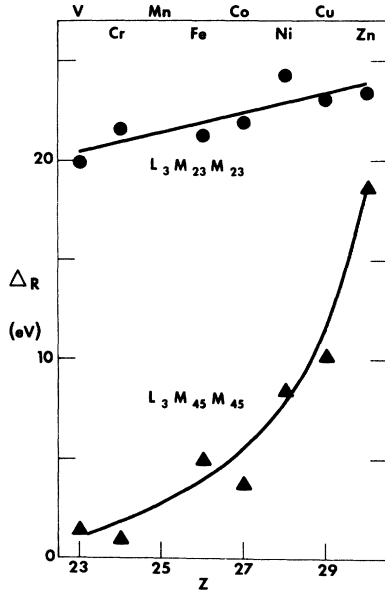


FIG. 6. Observed relaxation energy difference  $\Delta_R$  in eV vs atomic number  $Z$  for the transitions  $L_3 M_{23} M_{23}$  and  $L_3 M_{45} M_{45}$ .  $\Delta_R(L_3 M_{45} M_{45})$  decreases sharply with  $Z$  as a consequence of the delocalization of  $3d$  holes.

$$\Delta_R = \Delta_R^a + \Delta_R^{ea}.$$

Kowalczyk *et al.*<sup>4</sup> have pointed out that  $\Delta_R^{ea}$  may be approximated by  $F^0(3d, 4s)$  when the  $3d$  electrons are completely localized, because then the screening charge may be regarded as an electron of  $4s$  character drawn and localized on the double-hole atom of interest. In this approximation:

$$\Delta\epsilon(L_3 M_{45} M_{45}) = F^0(3d, 3d) - \Delta_R^a - F^0(3d, 4s). \quad (8)$$

The three terms on the right-hand side of Eq. (8) are all atomic in character even though they describe  $\Delta\epsilon$  in a solid. This is not surprising for solids whose  $3d$  electrons are completely localized such that the  $3d$  levels are essentially corelike

levels. To account for the delocalization of the  $3d$  electrons, we introduce the localization parameter  $\lambda_d$  so that

$$\Delta\epsilon(L_3 M_{45} M_{45}) = \lambda_d^2 [F^0(3d, 3d) - \Delta_R^a - F^0(3d, 4s)]. \quad (9)$$

Because delocalization is explicitly accounted for by  $\lambda_d^2$  in Eq. (9), we feel there is no need to use equivalent core approximations for the free-atom terms in the brackets.

The  $\Delta_R^a$  term for the  $L_3 M_{45} M_{45}$  transition is evaluated from two different sources. In the first approximation, we use the optical data tabulated by Moore.<sup>37</sup> Here the left-hand side of Eq. (6) is taken to be the ionization potential difference between a specific ion with initial  $3d^n 4s^0$  and  $3d^{n-1} 4s^0$  configurations. This difference is then subtracted from  $F^0(3d, 3d)$ ,<sup>33</sup> to obtain  $\Delta_R^a$  for a given element according to Eq. (6). These values are listed in Table V as  $\Delta_R^a$  (optical). It should be pointed out that in using  $3d^n 4s^0$  as an initial configuration, the atom is already once or twice ionized. However, the  $4s$  electrons are the outermost electrons, thus the effect of their absence on the ionization potential difference for the  $3d$  electrons is assumed to be small. Alternatively, one could also use the calculated values of  $\Delta_R^a$  of Gelius and Siegbahn as quoted by Kowalczyk *et al.*<sup>22</sup> In their notation  $\Delta_R^a$  is the static atomic relaxation energy which is equal to twice the dynamic relaxation energy  $E_R$  as calculated by Gelius and Siegbahn. These values are also listed in Table V as  $\Delta_R^a$  (theoretical). We see that  $\Delta_R^a$  obtained by the two methods do not differ from each other significantly.

Since  $\Delta_R^a$ ,  $F^0(3d, 3d)$ , and  $F^0(3d, 4s)$  are known in addition to the experimentally measured values of  $\Delta\epsilon(L_3 M_{45} M_{45})$ , we can calculate an approximate value of the localization parameter  $\lambda_d$  for the transition metals from Eq. (9). These results are given in Table V and shown in Fig. 5. Considering the approximations, the agreement of either cal-

TABLE V. Comparison of observed localization parameters  $\lambda_d$ (obs.) with those calculated from Eq. (9).  $\Delta_R^a$  is obtained either from optical (opt.) data or from theoretical (theor.) calculations of Gelius and Siegbahn quoted in Ref. 22. Experimental uncertainties are in parentheses. Interpolated values are starred.

$Z$	Metal	$\Delta\epsilon(L_3 M_{45} M_{45})$ (eV)	$F^0(3d, 3d)$ (eV)	$F^0(3d, 4s)$ (eV)	$\Delta_R^a$		$\lambda_d$ (calc.)		$\lambda_d$ (obs.)
					Opt.	Theor.	Opt.	Theor.	
23	V	0 (0.8)	18.7	8.7	3.2	5.0	0	0	0.28 (0.10)
24	Cr	1.3 (0.8)	18.4	8.2	3.9	(6.0)*	0.45	0.56	0.35 (0.11)
26	Fe	2.6 (0.8)	23.4	9.8	(6.0)*	7.8	0.58	0.67	0.57 (0.13)
27	Co	3.7 (0.8)	24.8	10.1	8.4	8.2	0.77	0.75	0.55 (0.14)
28	Ni	5.3 (0.8)	26.3	10.5	8.3	9.0	0.84	0.88	0.72 (0.14)
29	Cu	8.6 (0.3)	26.0	9.7	9.5	10.6	1.12	1.23	0.85 (0.17)
30	Zn	10.5 (0.3)	29.1	11.1	(11.0)*	10.6	1.22	1.19	1.00 (0.13)

culated values with experiment is quite satisfactory. As one might expect from the foregoing discussion, the calculated values indicate a systematic overestimation (larger  $\lambda_d$ ) of the localization of  $3d$  holes as well as the screening charges.

#### B. Total change in relaxation energy

As another alternative we may also calculate the total change in relaxation energy  $\Delta_R$  in the approximation scheme mentioned above. For the  $L_3M_{45}M_{45}$  transition, by comparing Eq. (9) with (4):

$$\Delta_R(3d, 3d) = \lambda_d^2 [\Delta_R^a + F^0(3d, 4s)]. \quad (10)$$

Using the  $\lambda_d$  derived from the  $S_{pd}$  data and the  $\Delta_R^a$  from either optical data or the theoretical calculations of Gelius and Siegbahn we obtain the set of  $\Delta_R$  (calc.) values listed in Table III. Again the systematically larger  $\Delta_R$  (calc.) values underscore the overestimation of the localized nature of extra-atomic relaxation in our approximation.

For the  $L_3M_{23}M_{23}$  transition one cannot use the same procedure to obtain  $\Delta_R^a$  from optical data. In this case the difference in ionization potential between the free ions of  $3p^63d^0$  and  $3p^53d^0$  configurations will be far greater than that of  $3p^63d^n$  and  $3p^53d^n$  owing to the high degree of ionization [e.g., Cr(VII) and Cr(VIII)]. Hence we only use the theoretical values of Gelius and Siegbahn as quoted by Kowalczyk *et al.*<sup>22</sup> The calculated total relaxation change  $\Delta_R$  (calc.) obtained this way (Table IV) compares quite satisfactorily with  $\Delta_R$  (obs.) and shows no systematic trend. We think this is because the  $L_3M_{23}M_{23}$  transition involves two truly localized electrons ( $\lambda_p = 1$ ) so that in this case the approximation of localized extra-atomic relaxation is much more realistic.

## VI. DISCUSSION

We have presented the detailed Auger spectra of the  $3d$  transition-metal series and attempted to quantitatively characterize them by the empirically derived energy and localization parameters  $\Delta\epsilon$  and  $\lambda$ . Previously, these Auger spectra of elements with open  $3d$  shells have not been studied in detail and it is extremely difficult to calculate or predict the extent of the delocalization of the  $3d$  electron. Now with the introduction of these two parameters, a physical understanding of the behavior of such Auger spectra, especially those involving  $3d$  band electrons, becomes possible. The salient points are summarized below.

(a)  $\lambda_d$  gives the quantitative extent of the delocalization of the  $3d$  electrons in metals with open  $3d$  shells. Because  $\lambda_d$  is derived from experiment, it is physically realistic.

(b) Through a knowledge of  $\lambda_d$  we are able, for the first time, to quantitatively isolate and estimate the respective contributions of (i) the hole-hole interaction, and (ii) the relaxation, to the total difference in energy  $\Delta\epsilon$  between single- and double-hole final states.

(c) It is evident from Fig. 4 that the main structure of the  $L_3M_{23}M_{45}$  transition remains unchanged as one moves from a filled  $d$  shell (Zn and Cu) to open  $d$  shells. Only the splitting  $S_{pd}$  decreases at a faster rate than that of the  $L_3M_{23}M_{23}$  structure ( $S_{pp}$ ) as the number of  $d$  electrons decrease and become more delocalized. This implies that the  $L_3M_{23}M_{45}$  transition retains its free-atom character throughout the transition series. The delocalization of  $d$  electrons (smaller  $\lambda_d$ ) serves to decrease the hole-hole interaction and decrease the relaxation change ( $\Delta_R$ ), but not sufficient to bring the band influence into this transition. Looking at it another way, because the considerable difference in screening between a  $3p$  (inner) hole and a  $3d$  (valence-band) hole, the energy change represented by  $\Delta\epsilon$  is almost entirely imparted to the  $3d$  electron alone. Thus even when the value of  $\Delta\epsilon(L_3M_{23}M_{45})$  is rather small (e.g., 2 eV for V), the  $3d$  electron can still be withdrawn from the band and a free-atom-like Auger structure results.

(d) For the  $L_3M_{45}M_{45}$  transition the situation is quite different. Here both electrons originate from the  $3d$  band. The net energy change represented by  $\Delta\epsilon(L_3M_{45}M_{45})$  is shared by both equivalent electrons in a one-step Auger process. Hence, unless  $\Delta\epsilon$  is quite large such as in Cu and Zn (9–10 eV) so that both  $3d$  electrons can be withdrawn from the band, for smaller values of  $\Delta\epsilon$ , this transition will retain its band character. This is not only evidenced by the decrease in  $\lambda_d$  with  $Z$  (Fig. 5), but also the rapid decrease in  $\Delta_R$  with  $Z$  (Fig. 6) indicating increased delocalization and very effective screening. We think this is likely to be the case from Co to V ( $\Delta\epsilon = 4-0$ ,  $\lambda_d = 0.5-0.3$ ) as shown by the large broadening in structure in the  $L_3M_{45}M_{45}$  group. Ni may be somewhat of a borderline case.

(e) In our discussion so far we have treated the structure of the Auger spectra exclusively in terms of the two-hole final state, be it free atom or bandlike. This is justified in the case of  $L_3MM$  transitions because the width of the initial  $L_3$  hole is small ( $\sim 0.5$  eV) compared to the  $3d$  band and the observed Auger structure, as discussed in Sec. III. Thus the  $L_3$  width does not contribute significantly to the width of the Auger lines. In the case of Coster-Kronig transitions of the type  $M_{1,2,3}VV$  the width of the initial vacancy is  $\sim 2$  eV for Cu and Zn,<sup>38</sup> and therefore can contribute significantly to the resulting Auger linewidths. Such

broadening caused by the initial vacancy width may make the interpretation of these Coster-Kronig spectra difficult.

(f) As expected the  $L_3M_{23}M_{23}$  structure remains free-atom-like throughout the series including As,<sup>31</sup> and Se.<sup>27</sup> The assignment of the two prominent peaks is generally thought to be  $^1D$  (left) and  $^3P$  (right) with the  $^1S$  (far left) too weak to be observed.<sup>1,27,31</sup> It is interesting to note, however, that the observed splitting of these two peaks  $S_{pp}$  is consistently a factor of 2 larger than the theoretical value<sup>30,33</sup> of  $\frac{6}{25}F^2(3p, 3p)$ , although it follows exactly the theoretical trend as a function of  $Z$ . (We note that this discrepancy has no effect on the localization parameter  $\lambda$ .) On the other hand, the observed splitting of  $S_{pd}$  for the  $L_3M_{23}M_{45}$  transition with filled  $3d$  shell ( $\lambda_d = 1$ ) agrees rather well with the theoretical value (e.g., for Cu the calculated and observed  $S_{pd}$  values are

7.7 and  $8.0 \pm 0.5$  eV, respectively, and for Zn, 8.5 and  $9.6 \pm 0.8$ , respectively). Furthermore, as shown in Fig. 4, the  $^1D$  peak of the  $L_3M_{23}M_{23}$  group becomes progressively broader with decreasing  $Z$  (unfilled  $3d$  bands) while the  $^3P$  peak shows the opposite trend. At present we do not know whether such behavior is due to many-body effects or some other mechanism.

#### ACKNOWLEDGMENTS

We gratefully acknowledge the helpful discussions with S. Seltzer and M. Mustafa and the able assistance of W. Lew with the experiments. One of us (T.T.) is grateful to the National Research Council and the National Academy of Science for a senior research associateship. At the University of Maryland this research is supported by the Center of Materials Research.

\*Permanent address: Physics Department, Howard University, Washington, D.C. 20059.

<sup>1</sup>L. Yin, T. Tsang, I. Adler, and E. Yellin, *J. Appl. Phys.* **43**, 3464 (1972).

<sup>2</sup>L. Yin, I. Adler, T. Tsang, M. H. Chen, and B. Crasemann, *Phys. Lett. A* **46**, 113 (1973).

<sup>3</sup>L. Yin, T. Tsang, I. Adler, and B. Crasemann, *Physica Fennica* **9**, S1, 256 (1974).

<sup>4</sup>S. P. Kowalczyk, R. A. Pollak, F. R. McFeely, L. Ley, and D. A. Shirley, *Phys. Rev. B* **8**, 2387 (1973).

<sup>5</sup>C. J. Powell, *Phys. Rev. Lett.* **30**, 1179 (1973).

<sup>6</sup>A. M. Baro, M. Salmeron, and J. M. Rojo, *J. Phys. F* **5**, 826 (1975).

<sup>7</sup>J. A. D. Mathew, J. D. Nuttall, and T. E. Gallon, *J. Phys. C* **9**, 883 (1976).

<sup>8</sup>P. Weightman, *J. Phys. C* **9**, 1117 (1976).

<sup>9</sup>M. H. Chen, B. Crasemann, L. Yin, T. Tsang, and I. Adler, *Phys. Rev. A* **13**, 1435 (1976).

<sup>10</sup>L. O. Werme, T. Bergmark, and K. Siegbahn, *Physica Scripta* **6**, 141 (1972).

<sup>11</sup>S. Hagmann, G. Hermann, and W. Mehlhorn, *Z. Phys.* **266**, 189 (1974).

<sup>12</sup>S. Aksela, J. Vayrynen, and H. Aksela, *Phys. Rev. Lett.* **33**, 999 (1974).

<sup>13</sup>H. Aksela and S. Aksela, *J. Phys. B* **7**, 1262 (1974).

<sup>14</sup>C. Bonnelle, in *Soft X-Ray Band Spectra*, edited by D. J. Fabian (Academic, New York, 1968), p. 163.

<sup>15</sup>R. C. Dobbyn, M. L. Williams, J. R. Cuthill, and A. J. McAlister, *Phys. Rev. B* **2**, 1563 (1970).

<sup>16</sup>R. G. Musket and R. J. Fortner, *Phys. Rev. Lett.* **26**, 80 (1971).

<sup>17</sup>G. F. Amelio and E. J. Scheibner, *Surf. Sci.* **11**, 242 (1968).

<sup>18</sup>L. Fey, F. R. McFeely, S. P. Kowalczyk, J. G. Jenkin, and D. A. Shirley, *Phys. Rev. B* **11**, 600 (1975).

<sup>19</sup>G. F. Amelio, *Surf. Sci.* **22**, 301 (1970).

<sup>20</sup>H. G. Maguire and P. D. Augustus, *J. Phys. C* **4**, L174 (1971).

<sup>21</sup>L. Yin, T. Tsang, and I. Adler, *Phys. Lett. A* **57**, 193 (1976).

<sup>22</sup>S. P. Kowalczyk, L. Ley, F. R. McFeely, R. A. Pollak, and D. A. Shirley, *Phys. Rev. B* **9**, 381 (1974).

<sup>23</sup>M. Salmeron, A. M. Baro, and J. M. Rojo, *Phys. Rev. B* **13**, 4348 (1976).

<sup>24</sup>D. A. Shirley, *Phys. Rev. B* **5**, 4709 (1972).

<sup>25</sup>L. Ley, S. P. Kowalczyk, F. R. McFeely, R. A. Pollak, and D. A. Shirley, *Phys. Rev. B* **8**, 2392 (1973).

<sup>26</sup>L. Yin, I. Adler, M. H. Chen, and B. Crasemann, *Phys. Rev. A* **7**, 897 (1973).

<sup>27</sup>P. Weightman, E. D. Roberts, and C. E. Johnson, *J. Phys. C* **8**, 550 (1975).

<sup>28</sup>C. D. Wagner, *Anal. Chem.* **47**, 1201 (1975); *Farad. Disc.* **60**, 291 (1976).

<sup>29</sup>R. E. Watson, M. L. Perlman, and J. F. Herbst, *Phys. Rev. B* **13**, 2358 (1976).

<sup>30</sup>J. C. Slater, *Quantum Theory of Atomic Structure* (McGraw-Hill, New York, 1960), Vol. 2.

<sup>31</sup>E. D. Roberts, P. Weightman, and C. E. Johnson, *J. Phys. C* **8**, 1301, 2336 (1975).

<sup>32</sup>E. J. McGuire, Sandia Laboratories Research Report SC-RR-710075 (unpublished, 1971).

<sup>33</sup>J. B. Mann, Los Alamos Scientific Laboratory Report LASL-3690 (unpublished, 1967).

<sup>34</sup>P. H. Citrin, J. E. Rowe, and S. B. Christman, *Phys. Rev. B* **14**, 2642 (1976).

<sup>35</sup>L. Hedén and A. Johansson, *J. Phys. B* **2**, 1336 (1969).

<sup>36</sup>D. A. Shirley, *Chem. Phys. Lett.* **16**, 220 (1972).

<sup>37</sup>C. E. Moore, *Atomic Energy Levels*, National Bureau of Standards Circular 467 (U.S. GPO, Washington, D.C., 1952).

<sup>38</sup>L. Yin, I. Adler, T. Tsang, M. H. Chen, D. A. Ringers, and B. Crasemann, *Phys. Rev. A* **9**, 1070 (1974).